Microvascular Research 85 (2013) 128–133

Contents lists available at SciVerse ScienceDirect

Microvascular Research

journal homepage: www.elsevier.com/locate/ymvre

Brief Communication

In vivo evaluation of venular glycocalyx during hemorrhagic shock in rats using intravital microscopy☆,☆☆

Ivo Torres Filho *, Luciana N. Torres, Jill L. Sondeen, I. Amy Polykratis, Michael A. Dubick

Damage Control Resuscitation, United States Army Institute of Surgical Research, Fort Sam Houston, TX 78234, USA

ARTICLE INFO

Article history:
Accepted 4 November 2012
Available online 12 November 2012

ABSTRACT

Hemorrhage is responsible for a large percentage of trauma-related deaths but the mechanisms underlying tissue ischemia are complex and not well understood. Despite the evidence linking glycocalyx degradation and hemorrhagic shock, there is no direct data obtained *in vivo* showing glycocalyx thickness reduction in skeletal muscle venules after hemorrhage. We hypothesize that damage to the endothelial glycocalyx is a key element in hemorrhage pathophysiology and tested the hypothesis that hemorrhage causes glycocalyx degradation in cremaster muscle microvessels. We utilized intravital microscopy to estimate glycocalyx thickness in 48 microvessels while other microvascular parameters were measured using non-invasive techniques. Systemic physiological parameters and blood chemistry were simultaneously collected. We studied 27 post-capillary venules (<16 μm diameter) of 8 anesthetized rats subjected to hemorrhage (40% of total blood volume). Six control rats were equally instrumented but not bled. Dextrans of different molecular weights labeled with FITC or Texas Red were injected. Glycocalyx thickness was estimated from the widths of the fluorescence columns and from anatomical diameter. While control rats did not show remarkable responses, a statistically significant decrease of about 59% in glycocalyx thickness was measured in venules after hemorrhagic shock. Venular glycocalyx thickness and local blood flow changes were correlated: venules with the greatest flow reductions showed the largest decreases in glycocalyx. These changes may have a significant impact in shock pathophysiology. Intravital microscopy and integrated systems such as the one described here may be important tools to identify mechanisms by which resuscitation fluids may improve tissue recovery and outcome following hemorrhage.

Introduction

Hemorrhage is responsible for a large percentage of trauma-related deaths in civilian and military settings but the mechanisms underlying tissue ischemia are complex and not well understood. In the last decade, the role of the vascular endothelium in maintaining vascular physiology and its role in vascular pathology, including hemorrhage, has begun to be better elucidated (Reitsma et al., 2007). The vascular endothelium plays a central role in regulation of permeability, the inflammatory response, the coagulation cascade, the anti-oxidant response, mechanotransduction changes of local blood flow (Pries and Kuebler, 2006). An integral component of the endothelial barrier is the endothelial glycocalyx. The glycocalyx is located on the apical surface of blood vessel's endothelial cell and is composed of membrane-spanning backbone molecules of proteoglycans, with associated side chain molecules made of glycosaminoglycans, and glycoproteins that are membrane bound (Reitsma et al., 2007; Weinbaum et al., 2007).

Intravital microscopy has been an invaluable resource for *in vivo* measurements of critically important parameters during hemorrhage/ischemia such as vessel diameter (Torres Filho et al., 2001a, 2001b), blood flow (Torres et al., 2008), functional capillary density (Top et al., 2011; Vazquez et al., 2011), oxygen partial pressure (Torres et al., 2008), microvascular permeability (Brookes et al., 2002) and blood cell–endothelium interactions (Lipowsky et al., 2011; Mulivor and Lipowsky, 2002, 2004). One of the challenges in studying alterations of the microcirculation *in vivo* following hemorrhage and trauma is the design and implementation of effective models to allow quantitative evaluations of systemic parameters while microcirculatory events are simultaneously recorded.

The *in vivo* study of the glycocalyx poses additional difficulties since its dimensions are close to the practical resolution limits of *in vivo* optical microscopy, requiring optimization of the available technology (Weinbaum et al., 2007). However, intravital microscopy has been successfully employed to study the endothelial glycocalyx (Smith et al., 2003; Vink and Duling, 1996). Considering the luminal distribution of circulating dextrans of different molecular weights, quantitative data on the dimensions and permeability characteristics of the glycocalyx has been provided (Cabrales et al., 2007; Vink and Duling,

☆ The material presented in this report is original and has not been submitted for publication elsewhere.
☆☆ This study complies with NIH guidelines for the care and use of laboratory animals.
* Corresponding author at: US Army Institute of Surgical Research, 3698 Chambers Pass, BHT-2, Room 282-2, Fort Sam Houston, TX 78234, USA. Fax: +1 210 539 6244.
E-mail address: ivo.p.torres.ctr@us.army.mil (I. Torres Filho).

0026-2862/$ – see front matter © 2012 Elsevier Inc. All rights reserved.
http://dx.doi.org/10.1016/j.mvr.2012.11.005

Report Documentation Page

Form Approved
OMB No. 0704-0188

1. REPORT DATE	2. REPORT TYPE	3. DATES COVERED
01 JAN 2013	**N/A**	**-**

4. TITLE AND SUBTITLE	5a. CONTRACT NUMBER
In vivo evaluation of venular glycocalyx during hemorrhagic shock in rats using intravital microscopy.	5b. GRANT NUMBER
	5c. PROGRAM ELEMENT NUMBER
6. AUTHOR(S)	5d. PROJECT NUMBER
Torres F. I. P., Torres L. N., Sondeen J. L., Polykratis I. A., Dubick M. A.,	5e. TASK NUMBER
	5f. WORK UNIT NUMBER
7. PERFORMING ORGANIZATION NAME(S) AND ADDRESS(ES)	8. PERFORMING ORGANIZATION REPORT NUMBER
United States Army Institute of Surgical Research, JBSA Fort Sam Houston, TX	
9. SPONSORING/MONITORING AGENCY NAME(S) AND ADDRESS(ES)	10. SPONSOR/MONITOR'S ACRONYM(S)
	11. SPONSOR/MONITOR'S REPORT NUMBER(S)

12. DISTRIBUTION/AVAILABILITY STATEMENT
Approved for public release, distribution unlimited

13. SUPPLEMENTARY NOTES

14. ABSTRACT

15. SUBJECT TERMS

16. SECURITY CLASSIFICATION OF:			17. LIMITATION OF ABSTRACT	18. NUMBER OF PAGES	19a. NAME OF RESPONSIBLE PERSON
a. REPORT	b. ABSTRACT	c. THIS PAGE			
unclassified	**unclassified**	**unclassified**	**UU**	**6**	

2000). The glycocalyx has been implicated in multiple physiological processes and diseases (Constantinescu et al., 2011; Reitsma et al., 2007; van den Berg et al., 2006). The glycocalyx degradation resulting from ischemia–reperfusion injury (Mulivor and Lipowsky, 2002, 2004; Rubio-Gayosso et al., 2006) is mediated by reactive-oxygen species (Rubio-Gayosso et al., 2006). Recently, glycocalyx degradation was reported in mesenteric venules after a severe, prolonged fixed-pressure model of hemorrhagic shock treated with lactated Ringer's solution and fresh frozen plasma (Kozar et al., 2011). However, those glycocalyx measurements were based on post-mortem electron microscopy images.

Despite the evidence linking glycocalyx degradation and hemorrhagic shock, there is no direct data obtained *in vivo* showing glycocalyx thickness reduction in skeletal muscle venules after hemorrhagic hypotension. We hypothesized that the venular endothelial glycocalyx of skeletal muscle is shed in response to a brief and mild fixed-volume hemorrhage model in rats. In order experimentally test this hypothesis we implemented an intravital microscopy system and a dual-fluorescent labeling technique with dextrans of different molecular weights to directly assess the glycocalyx *in vivo* before and after the hemorrhagic shock. We also assessed the correlation between glycocalyx changes and microvascular hemodynamics (centerline RBC velocity, blood flow) providing further insights into the effects of hemorrhagic shock on venular glycocalyx. Pertinent systemic parameters and glycocalyx changes of mesenteric venules were also studied.

Materials and methods

All protocols were approved in advance by the Institutional Animal Care and Use Committee of the US Army ISR. This study has been conducted in compliance with the Animal Welfare Act, the implementing Animal Welfare Regulations, and the principles of the Guide for the Care and Use of Laboratory Animals. Male Sprague–Dawley rats (Charles River Laboratories, Wilmington, MA, 220 ± 10 g body weight) breathing spontaneously room air or 100% oxygen were anesthetized with isoflurane (2%). Tracheostomy was performed to ensure a patent airway.

Systemic measurements

One carotid artery was cannulated (2-French Mikro-tip catheter transducer, model SPR-320, Millar Instruments, Houston, TX) for monitoring blood pressure. One femoral vein was used to infuse fluorescent dyes and other fluids, and one femoral artery was used for blood withdrawal and to collect blood samples. Total hemoglobin concentration, pH, lactate, base excess, bicarbonate, and K^+, were measured from blood samples (CG4, CHEM8 modules, I-stat, Abbott, Chicago, IL). Blood was collected into heparinized glass capillary tubes for hematocrit measurement (microhematocrit centrifuge model MB, Needthan HTS, MA). Hemoglobin O_2 saturation (SO_2) and respiratory rate (RR) were measured non-invasively (MouseOx, Starr Lifesciences). Arterial blood pressure, heart rate, core temperature, SO_2 and RR were monitored and continuously recorded using a computerized acquisition system (Dynamic Research Evaluation Workstation — DREW, US Army Institute of Surgical Research, San Antonio, TX, with DAQ module, Model USB 6218 BNC, National Instruments, Austin, TX) that also calculated the mean arterial blood pressure (MAP), systolic and diastolic blood pressures from the arterial blood pressure signal.

Intravital microscopy

The system was assembled over a horizontal breadboard anti-vibration table (63–533, TMC, Peabody, MA) to limit the vibrations from the floor that could degrade image quality. A fixed-stage upright microscope (BX51WI, Olympus) was equipped with dry objectives used for selecting the microvessels and all reported observations were made with an infinity corrected water immersion objective (Zeiss 63x, N.A. = 0.95). A 100 W tungsten-halogen lamp was used for transillumination and a Metal Halide was used for epi-illumination with selective filter block systems for Texas Red (TR) fluorescence (excitation and emission wavelength, 545–580 nm and >610 nm, respectively) and fluorescein isothiocyanate (FITC) fluorescence (excitation and emission wavelength, 470–495 nm and 510–550 nm). One optical exit of the microscope was connected to a velocity measuring device head (Optical Doppler Velocimeter, Texas A&M), a 3-CCD color camera (DXC-C33, Sony), a recorder (SR-HD1500US blu-ray disc & HDD recorder, JVC) and was also used to collect video segments for dynamic measurements such as leukocyte-endothelium interactions. The second exit was connected to a digital charge-coupled device (CCD) camera (CoolSnap cf; Roper Scientific, NJ) with 1392×1040 pixels resolution. The camera was computer-controlled and the generated images were digitally stored for later analysis. The microscope stage and the focus were adjusted manually.

Experimental animal preparations

In vivo experiments were performed on the exteriorized cremaster muscle and mesentery preparations, using a dual thermostatically-controlled transparent platform (Golub and Pittman, 2003), as previously described (Harris et al., 1975; Hutchins et al., 1973; Torres Filho et al., 2001a, 2001b). The cremaster was exteriorized by an incision made in the left scrotum and the muscle was positioned flat over a thin sapphire pedestal that was thermostabilized with a transparent heater and thermo controller (CT-698, Minco, Minneapolis, MN). During the surgical preparation, the muscle was bathed by warm Krebs–Henseleit solution that was discontinued after surgery. In order to prepare the mesentery, an ileal loop and respective mesentery were carefully exteriorized and the tissue was spread over the warmed transparent viewing platform. Any exposed gut was covered with gauze soaked in saline. After exposure, both preparations were covered with a thin impermeable plastic film (Saran Wrap, Dow Corning, Midland, MI) to minimize both dehydration and gas exchange with the atmosphere. The animal platform was then positioned over the microscope stage.

Fluorescently-labeled dextran (Dx) solutions

Since dextrans can be readily excluded from the glycocalyx under control conditions but can penetrate the glycocalyx after hemorrhage due to their size and charge, we used neutral Dx of different molecular weights (Dx40 = 40 kDa, Dx70 = 70 kDa, Dx500 = 500 kDa), labeled with either TR or FITC, to measure the space occupied by the glycocalyx. At baseline, TR–Dx70 and TR–Dx40 were injected for determining the intact glycocalyx thickness, followed by FITC–Dx70 and FITC–Dx500 during hemorrhagic shock. After each bolus of fluorescently labeled Dx was administered, 5 minutes was allowed for the fluorescence to reach a steady state level.

Experimental protocol

Initially, 2–4 microscopic fields containing post-capillary venules were randomly selected. Five minutes before baseline measurements, TR–Dx70 (10 mg/ml, Molecular Probes) was injected. Each field was recorded under transmitted light before epi-fluorescence illumination. Paired images of individual microvascular segments using each tracer were recorded using the CCD camera and transferred to a computer. TR–Dx40 (10 mg/ml) was then injected and the same paired recordings (transillumination followed by epi-illumination) were performed for each microvessel, in the exact positions as in the previous sequence. In order to minimize light exposure and excessive or undesirable probe excitation in studied and adjacent microvessels, the field diaphragm size and the duration of both epi-illumination and camera

exposure were reduced as much as possible. Both the transillumination and external light were switched off before the fluorescence recordings begun. Red blood cell velocity was determined on-line using an Optical Doppler Velocimeter (Borders and Granger, 1984; Davis, 1987). Blood flow and shear rate were calculated from RBC velocity and vessel diameter as described previously (Torres et al., 2008).

In order to reproduce a more realistic scenario, we used a recently published hemorrhagic shock model (Torres Filho et al., 2010) where the MAP was not kept at any pre-determined level. A fixed-volume hemorrhage was induced in 30 minutes using a double-lumen catheter (Braintree Scientific, Inc., Braintree, MA) for simultaneous bleeding and infusion of Na^+ citrate solution (Baxter Healthcare Corp., Deerfield, IL) for regional extracorporeal anticoagulation by means of 2 synchronized syringe pumps. The target shed blood volume was calculated as 40% of total blood volume. In a separate group of rats, a set of systemic measurements was performed at the end of the 30-min bleeding, to document the systemic effects of the hemorrhagic shock. After 90 minutes of shock period, FITC–Dx500 (10 mg/ml, Sigma) was injected and paired recordings of the selected fields were performed. Finally, FITC–Dx70 (10 mg/ml) was injected and paired recordings of all fields were made. A set of systemic parameters was collected during baseline coinciding with the microcirculatory data. A final set of systemic measurements was performed during the hemorrhagic shock period, also coinciding with the collection of microcirculatory data ($t=90$ min). Control animals were subjected to all procedures except hemorrhage.

Glycocalyx thickness measurements

To estimate the glycocalyx thickness, the dye-exclusion method (Henry and Duling, 1999) and the image analysis method pioneered by Gao and Lipowsky (2010) were adapted. As illustrated in Figs. S1 and S2 of Supplementary Material, the thickness was estimated from the widths of the fluorescent columns using epi-illumination images and from the microvessel inner diameter measured using transillumination images (herein called anatomical diameter, ***d***). A measurement line was traced, perpendicular to the longitudinal axis of each vessel. The line was of sufficient length to span the entire microvessel width and beyond. Its exact location was noted and used in all subsequent images at different time points (baseline and post-shock). The image analysis software produced a profile of the light intensity along this line. For transillumination images, the profile helped determine the anatomical diameter: the endothelial cell surface was taken as the outer edge of the dark refractive band present near the wall under brightfield transillumination. For epi-illumination images, the fluorescence intensity at the endothelial cell surface generated a sigmoidal curve: the inflection points in the dye intensity curves were taken as the outer edges of the glycocalyx. The difference between the inflection point and surface of the endothelial cell was taken as the glycocalyx thickness. All image processing and measurements were performed using Image-Pro Plus software (MediaCybernetics) and a high-resolution monitor (model U3011, Dell, at 2560×1600 pixels resolution) at a final magnification of approximately $2500\times$. The distance scale was calibrated by recording the image of a stage micrometer (10-μm divisions, at same magnification as video microscopic recordings). The scaling factor was 0.065 μm/pixel.

Statistics

The deviation from Gaussian distribution was tested for all systemic and microvascular data. Parametric tests were found adequate. Values are reported as mean ± SEM. Differences between before and after hemorrhage as well as between groups were analyzed by using repeated measures ANOVA. A level of $p<0.05$ was considered significant.

Results

Time control rats

Animals subjected to all procedures except hemorrhage showed relatively stable systemic parameters throughout the experimental period of 2 hours: the differences between baseline and "hemorrhage" values were not statistically significant (data not shown). Twenty-one post-capillary venules from 6 different preparations were studied in these animals. The mean anatomical diameter and red blood cell velocity did not show significant change over time for mesenteric or cremasteric post-capillary venules. Pooled average results are shown in Table 1.

In order to evaluate potential changes in glycocalyx thickness, fluorescently labeled dextrans were used. During baseline, the diameter of the fluorescent column of TR–Dx40 was not different from the anatomical diameter for the studied venules (Table 1). However, the difference between the anatomical diameter and the diameter of the fluorescent columns of TR–Dx70, FITC–Dx70 and FITC–Dx500 were all statistically significant. Therefore, in animals that were not subjected to hemorrhage, dextrans of low molecular weight (40 kDa) penetrated the glycocalyx but larger Dx (70 kDa and above) did not. The estimated glycocalyx thickness based on these differences did not change from baseline to post-"hemorrhage" period and averaged 0.772 ± 0.040 μm. These findings also suggested a small or minimal photobleaching/glycocalyx damage as a result of the light-dye treatment.

Hemorrhaged rats

Animals were bled by an average final volume of 23.3 ± 0.5 ml kg^{-1} and all rats survived the complete protocol. Table 2 shows the systemic parameters that were measured at the end of the hemorrhage period and at the time when the microcirculatory measurements were taken. In contrast with baseline, there were sharp changes in the systemic parameters at the end of the hemorrhage. In terms of venular RBC velocity and blood flow, there was a significant decrease to $52.7\pm13.4\%$ and $35.2\pm12.8\%$ of baseline, respectively. All microvascular data are summarized in Table 1.

Changes in glycocalyx thickness

In preliminary tests, 12 vessels from randomly selected experiments were measured by three investigators, only one of them not blinded with regards to the protocol/origin of the images. The 3 sets of results were not statistically different from each other (data not shown).

The diameter of the fluorescent column of TR–Dx40 during baseline was not different from the anatomical diameter (d). After hemorrhage, the difference between the anatomical diameter and the diameter of the fluorescent column of FITC–Dx70 was not statistically significant. Therefore, the slightly larger Dx70 penetrated the glycocalyx in animals that were subjected to hemorrhage. This was true for both mesentery and skeletal muscle preparations (Table 1).

Table 1
Microvascular parameters following hemorrhage.

Parameter	Control animals		Hemorrhagic shock animals	
	Baseline	Post-"hemorrhage"	Baseline	Post-hemorrhage
Diameter (μm)	15.1 ± 1.2	14.6 ± 1.2	14.1 ± 0.9	13.1 ± 1.0
Red blood cell velocity (mm/s)	1.7 ± 0.4	1.5 ± 0.4	1.4 ± 0.2	0.5 ± 0.1*
Blood flow (nl/s)	0.38 ± 0.12	0.32 ± 0.12	0.23 ± 0.06	0.04 ± 0.01*
Wall shear rate ($\times10^3$ s^{-1})	0.94 ± 0.21	0.85 ± 0.22	1.01 ± 0.23	0.36 ± 0.11*

Data expressed as mean ± SEM for 20 vessels from 6 control animals and 17 vessels from 7 hemorrhagic shock animals. Data from cremaster and mesentery preparations are pooled.
* Statistically significant ($p<0.01$) decrease after shock, compared to the baseline (same group) and to the control group at the same time point.

Table 2
Systemic parameters following hemorrhage.

Parameter	Baseline	Post-hemorrhage (T = 90 min)
Mean arterial pressure (mm Hg)	90.0 ± 4.0	56.5 ± 2.8
Pulse pressure (mm Hg)	34.1 ± 1.6	47.7 ± 3.2
O_2 saturation (%)	99.6 ± 0.1	99.5 ± 0.1
Heart rate (min^{-1})	329 ± 9	314 ± 12
Respiratory rate (min^{-1})	57 ± 5	79 ± 4
pH	7.368 ± 0.059	7.246 ± 0.046
Base excess (mmol/L)	0.1 ± 1.8	−4.8 ± 1.8
Bicarbonate (mmol/L)	27.8 ± 1.3	24.3 ± 1.8
Lactate (mmol/L)	1.2 ± 0.2	4.3 ± 0.8
Potassium (mmol/L)	4.2 ± 0.2	6.1 ± 0.3
Hematocrit (%)	36.2 ± 1.2	25.4 ± 0.1
Hemoglobin concentration (g/dL)	12.2 ± 0.5	8.7 ± 0.4

Data expressed as mean ± SEM for 7 animals.

The average glycocalyx thickness after hemorrhage for all 27 microvessels (0.155 ± 0.017 μm), estimated as half of the difference between the anatomical diameter and the width of the fluorescent column of Dx500 (d-FITC–Dx500) was 40.9 ± 6.0% of the baseline. This difference was statistically significant (Fig. 1). The change was also significant if compared to the control group. After hemorrhage, the glycocalyx thickness was reduced in 18 cremaster vessels to 0.148 ± 0.020 μm from a baseline of 0.477 ± 0.049 μm while the glycocalyx of 9 mesenteric venules reduced to 0.167 ± 0.033 μm from a baseline of 0.409 ± 0.049 μm. In addition, the changes in glycocalyx were positively correlated with both changes in venular RBC velocity ($r = 0.558$, $p < 0.05$) and with changes venular blood flow ($r = 0.640$, $p < 0.01$, Fig. 2).

Discussion

The results show, for the first time, the application of intravital microscopy to evaluate dynamic changes in the glycocalyx of living microvessels following hemorrhagic shock. The system was implemented to allow the acquisition of microvascular diameter and red blood cell velocity *in vivo* while blood sampling and systemic parameters (such as blood pressure, Hb O_2 saturation and respiratory rate) were simultaneously collected. Measurements of other important microcirculatory variables

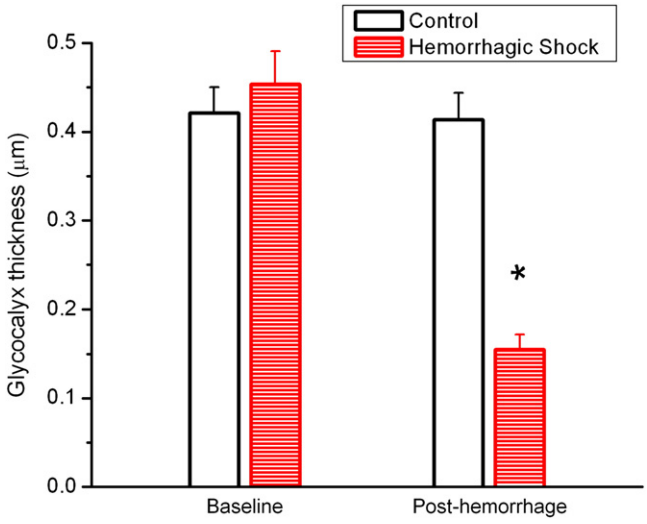

Fig. 1. Endothelial glycocalyx thickness measurements in post-capillary venules from cremaster and mesentery preparations. Rats not subjected to hemorrhage: "Control" group, 6 animals, 21 vessels. Rats bled by 40% of estimated total blood volume: "Hemorrhagic shock" group, 8 rats, 27 vessels. There was a statistically significant decrease in glycocalyx thickness after hemorrhage, compared to the baseline (same group) and to the control group at the same time point (*$p < 0.001$ on both cases). Data expressed as mean+SEM.

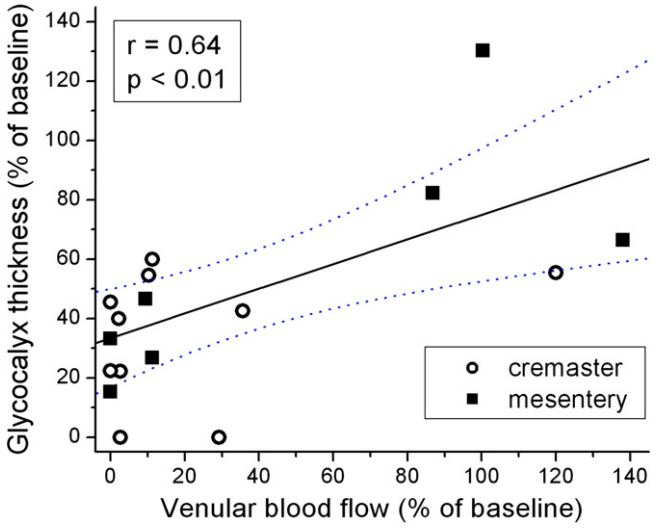

Fig. 2. Glycocalyx thickness measurements from 17 post-capillary venules during hemorrhagic shock, expressed as pre-hemorrhage values (baseline), as a function of the changes in venular blood flow (also calculated as percentage of baseline). Data pooled from 6 preparations. Solid line is the least squares best linear regression and dotted lines represent the 95% confidence interval. Correlation coefficient (r) and statistical significance (p) are also shown.

such as functional capillary density, PO_2 and hemoglobin O_2 saturation can be incorporated into the system. There is no commercially available system to allow a similar evaluation of physiological parameters *in vivo*.

In vivo glycocalyx changes were investigated in two different preparations (muscle and mesentery) because they provide complementary and useful information on pathophysiological aspects of hemorrhagic shock (Harris et al., 1975; Hutchins et al., 1973; Torres Filho et al., 2001a, 2001b). While skeletal muscle constitutes the largest component of the body mass, the mesentery is part of the splanchnic circulation and has advantages for intravital microscopy, in particular for microvessel permeability (Childs et al., 2007). Glycocalyx research has been performed using both tissues, such as the mouse cremaster (Rubio-Gayosso et al., 2006), but while the rat mesentery has been used to study responses to ischemia–reperfusion and inflammation (Lipowsky et al., 2011), the rat cremaster has never been used to evaluate the endothelial glycocalyx. The mesentery and skeletal muscle are unlike tissues not only in morphology, microvascular density and metabolic demand, but also structural remodeling of the resistance vasculature (Aird, 2007; Golub and Pittman, 2005; Torres et al., 2008) due to pathological conditions. Therefore, although venular glycocalyx did respond similarly between the two preparations this does not exclude the possibility that the mechanisms involved in the shedding may be different.

The results suggest that low MW dextrans penetrated the glycocalyx since measurements of TR–Dx40 (in baseline) and FITC–Dx70 (post-hemorrhage) widths were not statistically different from the anatomical diameter. Our estimations of baseline glycocalyx thickness are similar to the values obtained in vivo for mouse cremaster capillaries using transillumination (Constantinescu et al., 2011) but higher than the values reported for venules using fluorescent microparticle image velocimetry (Smith et al., 2003). After hemorrhage, a reduction of over 50% in glycocalyx thickness was measured. A recent review on the glycocalyx (Weinbaum et al., 2007) concluded that "we have only scratched the surface in determining its structure and function". Therefore, it is no surprise that almost no data exist on glycocalyx alterations following hemorrhage. To our knowledge, this is the first complete study using intravital microscopy showing degradation of glycocalyx in post-capillary venules after hemorrhagic shock. These results confirm our preliminary report using the rat spinotrapezius muscle (Torres Filho et al., 2009). In that study, image analysis of venular blood flow images

obtained *in vivo* suggested that hemorrhagic hypotension caused glycocalyx degradation. A more extensive study using post-mortem electron microscopy images recently showed that glycocalyx was reduced in mesenteric post-capillary venules of rats subjected to hemorrhagic shock and treated with lactated Ringer's (Kozar et al., 2011). Our current study presents *in vivo* data to suggest that the glycocalyx of post-capillary venules in the cremaster muscle show a similar effect following hemorrhagic shock. Taken together, these studies suggest that hemorrhage causes a widespread reduction in venular glycocalyx.

The impact of these changes in the pathophysiology of hemorrhagic shock is widely unknown. However, it is reasonable to consider that the magnitude of the changes may be significant since 50% or more of reduction in glycocalyx thickness was observed, both mesentery and skeletal muscle tissues were affected, and, if this effect is systemic, the overall vascular endothelial surface covered by the glycocalyx is potentially very large. Since the glycocalyx is involved in various processes at the microvascular level (Reitsma et al., 2007; Van Teeffelen et al., 2007; Weinbaum et al., 2007), it is reasonable to expect that these alterations are linked to the changes in microvascular permeability observed during hemorrhagic shock (Russell et al., 1995). It is also likely that the endothelial mechanotransduction of fluid shear stress is impaired (Weinbaum et al., 2007). Whether glycocalyx shedding is a relevant mechanism to promote neutrophil/leukocyte access to tissue during hemorrhagic shock and trauma is still a matter of debate. However, there is evidence to support this concept following ischemia and inflammation (Lipowsky et al., 2011; Mulivor and Lipowsky, 2002, 2004). Moreover, glycocalyx degradation by increased oxidative stress (oxidized LDL) stimulates leukocyte immobilization at the endothelial surface (Constantinescu et al., 2003).

Previous work in various species points towards a linkage between ischemia and glycocalyx degradation in heart (Becker et al., 2011; Chappell et al., 2011; Rehm et al., 2007), liver (van Golen et al., 2012) and mesentery (Mulivor and Lipowsky, 2004) in normovolemia. The *in vivo* data provided in the current work showing that greater glycocalyx decreases are correlated with larger reductions in blood flow (Fig. 2) confirm and expand this concept to hemorrhagic shock. However, in our protocol, the acquisition time points were fixed and glycocalyx thickness and blood flow were measured 90-min after the end of the blood removal. Therefore, it is not possible to ascertain whether glycocalyx was reduced at the onset of the low flow state or thickness decreased as a function of time during hemorrhagic shock.

Limitations

The technique of changes in glycocalyx permeability as a surrogate for the changes in thickness has been established for many years (Henry and Duling, 1999), and was adapted and applied for the current studies in a hemorrhagic shock model. However, a potential problem using the dye-exclusion technique is the application in vessels larger than 15 μm in diameter. In some cases, these vessels may present inhomogeneities and optical difficulties that may lower the resolution when measuring the fluorescent dye column (Weinbaum et al., 2007). In our study, we kept the microvessels on a fairly tight size range to avoid such errors but, in doing so, also restricted the range of studied vessels. We also limited the type of vessels although the methodology is suitable to arterioles and capillaries as well. There is recent evidence to support that glycocalyx changes occur in all types of microvessels in inflammation (Lipowsky et al., 2011). The endothelial glycocalyx structure includes various plasma proteins and soluble glycosaminoglycans tangled among the membrane bound elements. Since the reported measurements included the whole structure, without distinction between cell surface components and adsorbed proteins, it was not possible to identify which molecular components were more affected by the hemorrhage during the degradation process. For example, changes in plasma protein (content and/or composition) caused by hemorrhage may have resulted in changes in glycocalyx that could not be resolved by our methodology.

Conclusions

Intravital microscopy was successfully employed to estimate *in vivo* glycocalyx changes in post-capillary venules of rats subjected to hemorrhagic hypotension. The system was implemented in the same optical setup used for RBC velocity and microvessel diameter measurements, and allowed simultaneous recording of systemic physiological parameters. We showed that a significant reduction in glycocalyx thickness occurred in post-capillary venules of skeletal muscle and mesentery after hemorrhagic shock, especially those suffering large reductions in blood flow. These changes may have significant impact in shock pathophysiology. Various plasma proteins and soluble glycosaminoglycans are intertwined among the membrane bound elements within the endothelial glycocalyx structure. Therefore, future advances in resuscitation therapy for hemorrhagic shock will require detailed knowledge of the interplay between these fluids and the glycocalyx. The utilization of intravital microscopy and integrated systems such as the one described here may be important tools to help identify mechanisms by which resuscitation fluids may improve tissue recovery, survival and outcome following trauma and hemorrhagic shock.

Acknowledgments

The authors would like to thank M. Dale Prince, Daniel Darlington, Rodolfo DeGuzman, and Gary Muniz for their help during various phases of the study, James Aden for his help on statistical analysis, and Guy Drew (*in memoriam*) for his help with the computerized physiological data acquisition system. This study was supported in part by the US Army Combat Casualty Care Research Program, and was performed while the author Luciana Torres held a National Research Council Senior Research Associateship at the US Army Institute of Surgical Research and Ivo Torres Filho was employed by Premier Consulting & Management Services, Inc. and by Universidade do Estado do Rio de Janeiro (UERJ).

The views expressed herein are the private views of the authors and are not to be construed as representing those of the Department of Defense or the Department of the Army.

Appendix A. Supplementary data

Supplementary data to this article can be found online at http://dx.doi.org/10.1016/j.mvr.2012.11.005.

References

Aird, W.C., 2007. Phenotypic heterogeneity of the endothelium: II. Representative vascular beds. Circ. Res. 100, 174–190.
Becker, B.F., et al., 2011. Inosine, not adenosine, initiates endothelial glycocalyx degradation in cardiac ischemia and hypoxia. Nucleosides Nucleotides Nucleic Acids 30, 1161–1167.
Borders, J.L., Granger, H.J., 1984. An optical doppler intravital velocimeter. Microvasc. Res. 27, 117–127.
Brookes, Z.L., et al., 2002. Response of the rat cremaster microcirculation to hemorrhage in vivo: differential effects of intravenous anesthetic agents. Shock 18, 542–548.
Cabrales, P., et al., 2007. Microvascular and capillary perfusion following glycocalyx degradation. J. Appl. Physiol. 102, 2251–2259.
Chappell, D., et al., 2011. Sevoflurane reduces leukocyte and platelet adhesion after ischemia–reperfusion by protecting the endothelial glycocalyx. Anesthesiology 115, 483–491.
Childs, E.W., et al., 2007. Apoptotic signaling induces hyperpermeability following hemorrhagic shock. Am. J. Physiol. Heart Circ. Physiol. 292, H3179–H3189.
Constantinescu, A.A., et al., 2003. Endothelial cell glycocalyx modulates immobilization of leukocytes at the endothelial surface. Arterioscler. Thromb. Vasc. Biol. 23, 1541–1547.
Constantinescu, A., et al., 2011. Degradation of the endothelial glycocalyx is associated with chylomicron leakage in mouse cremaster muscle microcirculation. Thromb. Haemost. 105, 790–801.

Davis, M.J., 1987. Determination of volumetric flow in capillary tubes using an optical Doppler velocimeter. Microvasc. Res. 34, 223–230.
Gao, L., Lipowsky, H.H., 2010. Composition of the endothelial glycocalyx and its relation to its thickness and diffusion of small solutes. Microvasc. Res. 80, 394–401.
Golub, A.S., Pittman, R.N., 2003. Thermostatic animal platform for intravital microscopy of thin tissues. Microvasc. Res. 66, 213–217.
Golub, A.S., Pittman, R.N., 2005. Erythrocyte-associated transients in PO2 revealed in capillaries of rat mesentery. Am. J. Physiol. Heart Circ. Physiol. 288, H2735–H2743.
Harris, P.D., et al., 1975. Small vessel constriction in the rat cremaster during the early phase of moderate hemorrhagic hypotension. Microvasc. Res. 10, 29–37.
Henry, C.B., Duling, B.R., 1999. Permeation of the luminal capillary glycocalyx is determined by hyaluronan. Am. J. Physiol. 277, H508–H514.
Hutchins, P.M., et al., 1973. Effects of hemorrhagic shock on the microvasculature of skeletal muscle. Microvasc. Res. 5, 131–140.
Kozar, R.A., et al., 2011. Plasma restoration of endothelial glycocalyx in a rodent model of hemorrhagic shock. Anesth. Analg. 112, 1289–1295.
Lipowsky, H.H., et al., 2011. Shedding of the endothelial glycocalyx in arterioles, capillaries, and venules and its effect on capillary hemodynamics during inflammation. Am. J. Physiol. Heart Circ. Physiol. 301, H2235–H2245.
Mulivor, A.W., Lipowsky, H.H., 2002. Role of glycocalyx in leukocyte–endothelial cell adhesion. Am. J. Physiol. Heart Circ. Physiol. 283, H1282–H1291.
Mulivor, A.W., Lipowsky, H.H., 2004. Inflammation- and ischemia-induced shedding of venular glycocalyx. Am. J. Physiol. Heart Circ. Physiol. 286, H1672–H1680.
Pries, A.R., Kuebler, W.M., 2006. Normal endothelium. Handb. Exp. Pharmacol. 1–40.
Rehm, M., et al., 2007. Shedding of the endothelial glycocalyx in patients undergoing major vascular surgery with global and regional ischemia. Circulation 116, 1896–1906.
Reitsma, S., et al., 2007. The endothelial glycocalyx: composition, functions, and visualization. Pflugers Arch. 454, 345–359.
Rubio-Gayosso, I., et al., 2006. Reactive oxygen species mediate modification of glycocalyx during ischemia–reperfusion injury. Am. J. Physiol. Heart Circ. Physiol. 290, H2247–H2256.
Russell, D.H., et al., 1995. Hemorrhagic shock increases gut macromolecular permeability in the rat. Shock 4, 50–55.
Smith, M.L., et al., 2003. Near-wall micro-PIV reveals a hydrodynamically relevant endothelial surface layer in venules in vivo. Biophys. J. 85, 637–645.
Top, A.P., et al., 2011. The microcirculation of the critically ill pediatric patient. Crit. Care 15, 213.
Torres Filho, I.P., et al., 2001a. Vasomotion in rat mesentery during hemorrhagic hypotension. Life Sci. 68, 1057–1065.
Torres Filho, I.P., et al., 2001b. Effects of hypertonic saline solution on mesenteric microcirculation. Shock 15, 353–359.
Torres Filho, I.P., Vink, H., Torres, L.N., Pittman, R.N., 2009. Reduction in endothelial glycocalyx thickness after hemorrhage. FASEB J. 23, 950.
Torres Filho, I.P., et al., 2010. Early physiologic responses to hemorrhagic hypotension. Transl. Res. 155, 78–88.
Torres, L.N., et al., 2008. Microvascular blood flow and oxygenation during hemorrhagic hypotension. Microvasc. Res. 75, 217–226.
van den Berg, B.M., et al., 2006. Glycocalyx and endothelial (dys) function: from mice to men. Pharmacol Rep. 58 (Suppl.), 75–80.
van Golen, R.F., et al., 2012. Mechanistic overview of reactive species-induced degradation of the endothelial glycocalyx during hepatic ischemia/reperfusion injury. Free Radic. Biol. Med. 52, 1382–1402.
Van Teeffelen, J.W., et al., 2007. Endothelial glycocalyx: sweet shield of blood vessels. Trends Cardiovasc. Med. 17, 101–105.
Vazquez, B.Y., et al., 2011. Vasoactive hemoglobin solution improves survival in hemodilution followed by hemorrhagic shock. Crit. Care Med. 39, 1461–1466.
Vink, H., Duling, B.R., 1996. Identification of distinct luminal domains for macromolecules, erythrocytes, and leukocytes within mammalian capillaries. Circ. Res. 79, 581–589.
Vink, H., Duling, B.R., 2000. Capillary endothelial surface layer selectively reduces plasma solute distribution volume. Am. J. Physiol. Heart Circ. Physiol. 278, H285–H289.
Weinbaum, S., et al., 2007. The structure and function of the endothelial glycocalyx layer. Annu. Rev. Biomed. Eng. 9, 121–167.